Renewable and Sustainable Energy Reviews 16 (2012) 4982–4993

Contents lists available at SciVerse ScienceDirect

Renewable and Sustainable Energy Reviews

journal homepage: www.elsevier.com/locate/rser

Control strategies for single-phase grid integration of small-scale renewable energy sources: A review ☆

Mohammad Monfared [a,*], Saeed Golestan [b]

[a] Department of Electrical Engineering, Faculty of Engineering, Ferdowsi University of Mashhad, P.O. Box 91779-48974, Mashhad, Iran
[b] Department of Electrical Engineering, Abadan Branch, Islamic Azad University, Abadan, Iran

ARTICLE INFO

Article history:
Received 21 February 2012
Received in revised form
5 April 2012
Accepted 6 April 2012
Available online 27 June 2012

Keywords:
Small scale renewable energy sources
Single-phase grid integration
Control

ABSTRACT

Small-scale renewable energy sources, such as small hydro turbines, roof-mounted photovoltaic and wind generation systems, and commercially available fuel cells are usually connected to the single-phase distribution grid through a voltage source converter. To regulate the power exchange with the single-phase grid, and at the same time, reduce the harmonic distortions in the ac current, different current control structures have already been proposed, among which the current hysteresis control, the voltage oriented control, and the proportional-resonant based control have found more attentions. This paper provides an overview of the main characteristics of these control strategies. Also, some implementation aspects such as the fictitious signal generation and the single-phase grid synchronization techniques are discussed. Finally, through extensive simulations a comparative study of the presented control strategies is presented. The simulations are supported by experiments.

Contents

1. Introduction

Addressing the ever increasing global demand on reliable and sustainable electricity has become a main concern of electricity sector. At the moment, fossil fuel power plants are the backbone of world's electricity generation system. On the other hand, they are recognized as a major cause for the environmental pollutions [1]. Today, millions are willing to enjoy the benefits of improved lifestyle and environment with much more electricity generated from the renewable energy sources [2,3]. In 2010, renewable energies accounted for 16.6% of the world's primary energy demand, while a share up to 50% worldwide is feasible by 2040, according to a report published by the European Renewable Energy Council (EREC) together with its member associations (EPIA, ESHA, ESTIF, EUBIA, EUREC Agency, EWEA, AEBIOM and EGEC) [4].

☆ This paper has not published or submitted to conference or journal.
* Corresponding author. Tel.: +98 5118805073.
E-mail addresses: m.monfared@um.ac.ir (M. Monfared), s.golestan@ieee.org (S. Golestan).

1364-0321/$ - see front matter © 2012 Elsevier Ltd. All rights reserved.
http://dx.doi.org/10.1016/j.rser.2012.04.017

Nomenclature

I_d	active power current component
I_q	ractive power current component
i	ac current
k_p	proportional gain
k_i	integral or resonant gain
L	smoothing filter inductance
R	smoothing filter resistance
ζ	damping ratio
ω_n	natural frequency
ω_f	fundamental frequency
ω_{ff}	nominal value of fundamental frequency
P	Cauchy principal value
f_s	switching frequency
T_f	fundamental period
S_{error}	absolute percentage power error

Along with ambitious plans to increase the share of renewable energies in developed countries, such as EU 2020 political renewable energy goal [5], and progresses in renewable energy utilization in developing and newly industrializing countries [6–14], small-scale electricity generation systems, such as small hydro turbines, roof-mounted photovoltaic and wind generation systems, and commercially available fuel cells are being widely utilized at the distribution level [15,16]. The general structure of a small-scale renewable energy source, which is usually interfaced with the single-phase grid through a stage of power electronic devices, is depicted in Fig. 1. The source-side power conversion system extracts the maximum electricity from the available renewable input power and its topology and control strategy highly depends on the type of the renewable energy source. The focus of this paper is on the grid-side converter. The main objective of the grid-side converter is to control the power flow between the ac system and the dc link powered from the renewable resources. The single-phase voltage source converter (VSC) is the best solution for interfacing with a single-phase grid. It offers several advantages such as bidirectional power flow capability and low distortions at the ac side current and the dc side voltage. Another promising feature is that it can independently control the active and reactive power exchanged with the ac network; therefore, it can improve the voltage profile, and is able to operate in weak ac systems. These advantages make the single-phase VSC a successful solution for grid integration of small-scale renewable energy sources.

To regulate the power exchange with the single-phase grid, and at the same time, reduce the harmonic distortions in the ac current, different current control structures have already been proposed, such as current hysteresis control (CHC) [17–26], voltage oriented control (VOC) [27–31], and proportional-resonant (PR) based control [32–39], which all have their own pros and cons.

This paper gives an overview of the main characteristics of these control strategies. The paper also includes a discussion of some implementation aspects such as the fictitious signal generation and the single-phase grid synchronization techniques. Then, through extensive simulations a comparative study of the presented control strategies is presented and discussed. The simulations are supported by experiments.

2. Control strategies for single-phase grid-tie converters

Advanced power control strategies for single-phase converters imitate the concept of decoupled active and reactive power control of three-phase converters which is realized in the synchronous reference frame. In this way, the ac current is decoupled into active and reactive power components, I_d and I_q, respectively. These current components are then regulated in order to eliminate the error between the reference and measured values of the active and reactive powers. In most cases, the active power current component, I_d, is regulated through a dc-link voltage control aiming at balancing the active power flow in the system. As shown in Fig. 1, the power control loop is followed by a current control system. By comparing the reference and measured currents, the current controller should generate the proper switching states for the converter to eliminate the current error and produce the desired ac current waveform. It is worth mentioning that, for the sake of simplicity, in the converter of Fig. 1, a simple L-type smoothing filter is shown. However, a higher order LC or LCL filter brings improved harmonic suppression performance at lower switching frequencies with a reduction of overall filter size, but at the expense of probability of resonance. Yet, it is possible to

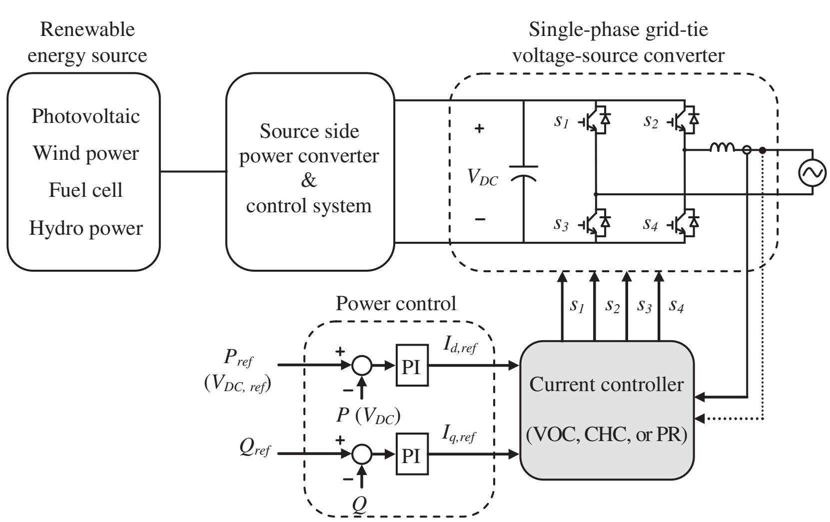


Fig. 1. Block-diagram of a renewable energy source interfaced with the single-phase grid.

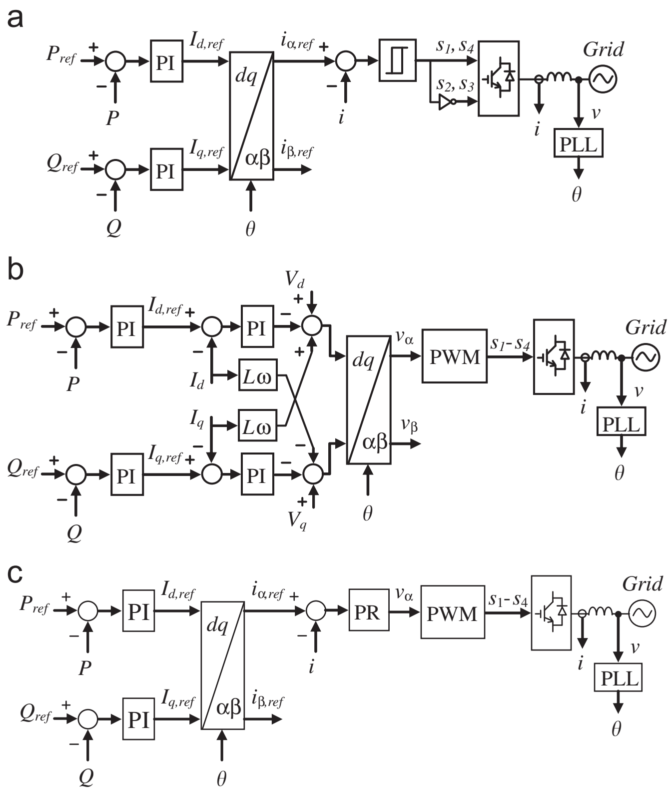


Fig. 2. Simplified block-diagram of (a) CHC, (b) VOC and (c) PR-based control of single-phase grid-tie converters.

employ a single loop current controller, which is the scope of this paper, to these higher order converter systems. Recently, the idea of multi-loop current control is developed for three-phase converters with LC and LCL filters to improve the system stability and resonant damping. This technique is also adopted for single-phase applications [38–41].

The performance of the converter system mostly depends on the quality of the current control strategy. Among different single loop current control strategies, CHC, VOC, and PR have received more attentions in recent years. The basic structures of these techniques are depicted in Fig. 2 and are discussed in the following subsections. It is noteworthy that in addition to the three above mentioned control strategies, some novel approaches based on predictive [42–44], fuzzy logic [45], artificial neural networks [46], sliding mode [47,48], and digital repetitive control [41,49–53] are presented in the literature. All these techniques try to maintain the advantages of conventional current control structures, especially precise current control with minimum distortion and harmonic noises at the expense of difficult design and implementation, more computational burden and the requirement of a good knowledge of the system parameters.

2.1. Current hysteresis control (CHC) [17–26]

The CHC is one of the easiest control strategies, in which, the ac current is controlled to stay within the limits of an upper and lower bands around the sinusoidal reference current. For this purpose, the hysteresis controller is used which is simple and provides a high dynamics. The output of the hysteresis controller is the converter switching states, so in CHC there is no PWM modulator block, which simplifies the structure and improves the dynamics. Despite the advantages of simplicity, robustness, good stability, automatic current limiting, and high dynamic response, the basic CHC suffers from major drawbacks such as, widely varying switching frequency and large current ripples. Indeed, the switching frequency depends on the hysteresis bandwidth, the sampling frequency, and system and load parameters and varies over a wide range. As a consequence, significant low-order harmonics are present in the ac current and it is important to carefully design the filter as well as the converter power stage. Besides, the high gain of the hysteresis controller may cause some control difficulties or power quality problems, especially when the filter inductance and/or the sampling frequency are small. It is worth mentioning that some advanced CHC structures have been proposed which use an adaptive band for the controller and could obtain a fixed switching frequency [25,26]. This is at the expense of deteriorated performance characteristics, such as increased current harmonic distortions, degraded dynamics and lower stability margins.

2.2. Voltage oriented control (VOC) [27–31]

The voltage-oriented control or VOC is a well-known method of indirect active and reactive current control and is based on the current vector orientation with respect to the line voltage vector. The VOC is realized in the direct-quadrature (dq) synchronous reference frame, where the error between the direct (I_d) and quadrature (I_q) components of the ac current and their reference values are fed to the PI controllers. Then, the controllers generate the reference voltage for the converter. This voltage is applied to the converter using a PWM modulator. Compared with the CHC, the converter switching frequency is fixed and by using advanced modulation techniques, the switching losses, harmonic currents and total harmonic distortion (THD) can be minimized. Also, thanks to the internal current control loops, high dynamics and static performance is guaranteed. One main drawback associated to the VOC is that the performance is highly dependent on the applied current control strategy and the connected ac network conditions.

As one can see in Fig. 2(b), in the VOC, electrical signals are all transformed to the synchronous reference frame, where quantities are dc and, as a consequence the zero steady-state error is ensured by using a conventional proportional-integral (PI) controller. This transformation needs at least two orthogonal signals. As a consequence, a fictitious phase must be generated. To create a two phase system from a single phase signal, different techniques can be employed, such as the transport delay [54], Hilbert transformation [55,56], all-pass filter (APF) [57], and SOGI [58] methods. These techniques are presented in the next section.

2.2.1. VOC design considerations

The transfer function of a PI controller is as (1), in which k_p and k_i are the proportional and integral gains, respectively.

$$PI(s)=k_P+k_is \tag{1}$$

If the converter model in Fig. 2(b) is simplified to $1/(Ls+R)$, where L and R are the filter inductance and resistance, respectively, and assuming that the cross-couplings are eliminated by using the decoupling terms ($L\omega I_d$ and $-L\omega I_q$), then the closed-loop transfer function of the d and q current loops can be readily derived as

$$\frac{I_d(s)}{I_{d,ref}(s)}=\frac{I_q(s)}{I_{q,ref}(s)}=\frac{k_ps+k_i}{Ls^2+(k_p+R)s+k_i} \tag{2}$$

where I_{dq} and $I_{dq,ref}$ are the measured and reference currents, respectively. Comparing (2) with the standard second-order characteristic equation and assuming that $k_i \gg k_p$, the damping

ratio (ζ) and the natural frequency (ω_n) are calculated as

$$\zeta = \frac{k_p + R}{2\sqrt{k_i L}} \tag{3}$$

$$\omega_n = \sqrt{\frac{k_i}{L}} \tag{4}$$

Hence, the current controller gains will be designed as

$$k_P = 2\zeta\omega_n L - R \tag{5}$$

$$k_i = L\omega_n^2 \tag{6}$$

Obviously, the choice of controller gains is a compromise between the stability margin and the dynamic performance.

2.3. PR-based control [32–39]

It is well-known that, in spite of its popularity, a PI controller is not able to track a sinusoidal reference without the steady-state error (both magnitude and phase). Also it suffers from the poor disturbance rejection capability. Consequently, it is not common and not recommended at all, to employ a PI controller with ac signals.

To overcome the aforementioned problems of conventional PI controllers in the stationary reference frame, some complicated control structures are proposed. The most recent is based on the type III compensator [59] with the transfer function of

$$G(s) = k\frac{(s+z_1)(s+z_2)}{s(s+p_1)(s+p_2)} \tag{7}$$

As the CHC method, it is also performed in the stationary reference frame and no coordinate transformation is needed in the current control loop. As shown in (7), the controller has three poles and two zeros with one pole placed at the origin. Two zeros are located around the fundamental frequency to compensate the drop in phase, and two poles are used to attenuate the high frequency disturbances. Yet, with the added complexity, no satisfactory improvement in the steady-state performance and harmonics rejection is obtained.

A successful method for current control of grid connected converters in the stationary reference frame, is the proportional-resonant (PR) based control. The transfer function of a PR controller is as

$$PR(s) = k_P + k_i\frac{s}{s^2 + \omega_f^2} \tag{8}$$

where k_p and k_i are the proportional and resonant gains, respectively, and ω_f is the fundamental frequency. As clear in (8), unlike the PI controller which has a very high gain at the zero frequency, the PR controller provides such a high gain around the fundamental frequency of the ac system (resonant frequency), assuring a zero steady-state error when regulating sinusoidal signals. Ideally, other frequencies are not affected. So, it exhibits an exceptional ability to compensate voltage harmonics in a selective way. For this purpose, the basic PR controller of (8) can be easily extended by adding more resonant terms tuned at the desired harmonic frequencies ($n\omega_f$), as

$$PR(s) = k_P + k_i\frac{s}{s^2 + \omega_f^2} + \sum_{n=3,5,\ldots} k_n\frac{s}{s^2 + (n\omega_f)^2} \tag{9}$$

where k_n is the resonant gain at the nth-order harmonic. Besides its simplicity, the system dynamics is almost not affected by the harmonic compensation terms. It is an interesting feature of the PR controller and makes it a promising candidate for the applications where high system dynamics and harmonics compensation are required at the same time.

On the other hand, despite its simplicity, ease of low-order voltage harmonics compensation, and high dynamics, the PR-based control has several disadvantages, such as sensitivity to system frequency variations, and great sensitivity and possibility of instability to the phase shift of current sensors.

2.3.1. PR-based design considerations

Again, with $1/(Ls+R)$ as the converter model in Fig. 2(c), the closed-loop transfer function of the current loop can be obtained as

$$\frac{i(s)}{i_{\alpha,ref}(s)} = \frac{k_p s^2 + k_i s + k_p\omega_f^2}{Ls^3 + (k_p+R)s^2 + (k_i + L\omega_f^2)s + (R+k_p)\omega_f^2} \tag{10}$$

where i and $i_{\alpha,ref}$ are the measured and reference currents, respectively. Due to the high complexity of the closed loop system, introduced by the PR structure, the controller design is not as straightforward as the procedure used for the system described by (2). In practice, simulation techniques are used to determine the values of the proportional and resonant terms. As some general guidelines, the integral gains determine the control bandwidths centered at the relevant harmonic frequencies. The integral gains should be minimized to ensure that each resonant term does not affect other frequencies. However, these gains may be oversized according to the expected fundamental frequency variations. Also, the proportional gain, k_p, has the same function as the proportional term in the PI controller.

On the other hand, the highest order harmonic (n_{max}) which can be included in the harmonics compensation network must have a frequency enough smaller than the crossover frequency of the open loop system. The crossover frequency is mainly determined by k_p and is restricted by the required stability margin. In most applications, the maximum accessible crossover frequency limits the compensation terms to fifth or seventh-order harmonics.

3. An overwiew of fictitious phase generation techniques

The single-phase circuit has one phase conductor with a neutral return. In order to extend the stationary (αβ) or synchronous (dq) reference frame control strategies to single-phase systems, at least two orthogonal signals are necessary. So, a second fictitious phase should be properly generated to model a single-phase circuit as an equivalent virtual two-phase circuit.

In the literature, there are several successful works for generating the fictitious phase including the transport delay [54], Hilbert transformation [55,56], all-pass filter [57], and SOGI [58] methods.

In the transport delay method, shown in Fig. 3, a phase shift of 90° with respect to the fundamental frequency of the input signal is realized through the use of a first-in-first-out memory, with the delay adjusted to one fourth the number of total samples of a cycle of the fundamental frequency. This method is simple and can be readily implemented by digital controllers without the need for tuning any parameters. Due to one quarter cycle delay in the second phase, the controller cannot respond to changes in the system immediately. Poor performance in the presence of frequency fluctuations is other major drawback of this technique [58].

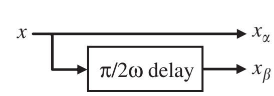


Fig. 3. Transport delay method to generate the fictitious phase signal.

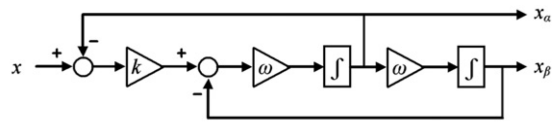


Fig. 4. SOGI method to generate the fictitious phase signal.

The Hilbert transformation is defined as (11), where P is Cauchy principal value.

$$x_\beta(t) = \frac{P}{\pi}\int_{-\infty}^{\infty}\frac{x(\tau)}{t-\tau}d\tau \tag{11}$$

Due to great sensitivity to input disturbances and frequency fluctuations, it has found no industrial acceptance. On the other hand, the original transformation shown in (11) brings noncausality and is not practically realizable. The modifications proposed for Hilbert transformation are mainly based on finite impulse response (FIR) and infinite impulse response (IIR) filters which their implementation imposes a high computational burden on the control system [60].

An all-pass filter (APF) approximates the response of the Hilbert transformation and can be easily implemented in discrete platforms and has been proven to be an attractive solution. Usually the second phase is implemented by using a first-order APF with the following transfer function

$$H(s) = \frac{\omega_f - s}{\omega_f + s} \tag{12}$$

where ω_f is the fundamental angular frequency.

A recently developed technique, illustrated in Fig. 4 is based on the second-order generalized integrator (SOGI) which besides its simple structure provides filtering. The gain k is adjusted according to the needed level of filtering and x_α is the filtered x. It should be noted that a proper filtering of the grid voltage brings a clean template for synchronization and power calculations. However, an extensive filtering of ac current may cause external disturbances (such as line and load disturbances) do not effectively contribute to the closed loop current control system. This can result in a poor tracking and disturbance rejection performance under distorted grid conditions and degraded dynamic response or even instability at transients.

Apparently, all fictitious phase generation techniques are frequency dependent, so problems can occur when the grid frequency has fluctuations. Usually these techniques receive a frequency feedback from the PLL block to boost the performance.

4. An overwiew of single-phase grid synchronization techniques

A lot of synchronization techniques, for both single-phase and three-phase applications, are available in the literature [61]. Thanks to their simplicity, robustness, and effectiveness, the phase locked loops (PLLs) are the most accepted ones. Generally speaking, a PLL is a closed loop feedback control system, which synchronizes its output signal in phase, as well as in frequency, with the fundamental component of the grid voltage. Among various techniques, currently, the synchronous reference frame PLL (SRF-PLL) is more employed. As illustrated in Fig. 5 the main difference between different single-phase SRF-PLL structures is in how the fictitious phase generator in the phase detector block is implemented. Accordingly, single-phase PLLs are mainly divided into the transport delay-based, Hilbert transformation-based, all-pass filter-based, and SOGI PLL [58,62–65]. In Fig. 5, a feedforward of the nominal value of the fundamental frequency, denoted as

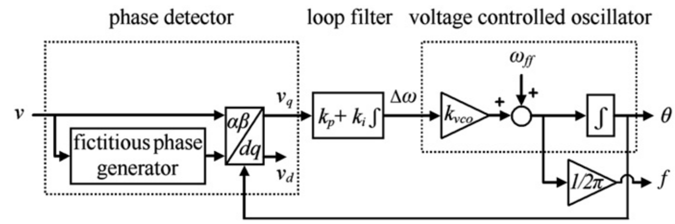


Fig. 5. Block diagram of a single-phase PLL (usually referred to as the synchronous reference frame PLL).

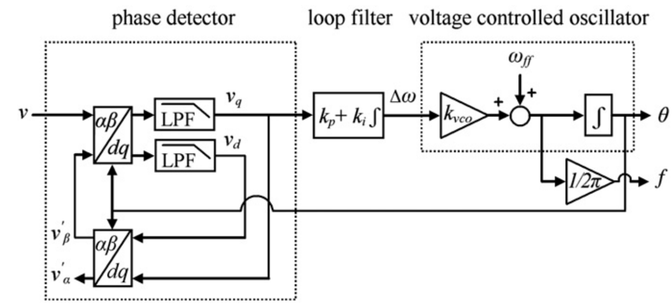


Fig. 6. Block diagram of the inverse Park PLL.

Table 1
System parameters.

Parameter	Value
Nominal power (kVA)	1
DC link voltage (V)	200
Grid voltage (Vrms)	70
Grid frequency (Hz)	50
Filter inductance (mH)	3.7
Filter resistance (mΩ)	250
Sampling frequency (kHz)	5
Switching frequency (kHz)	5

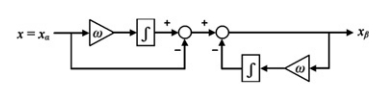


Fig. 7. Block diagram representation of the first-order APF (Eq. (12)).

ω_{ff}, reduces the control effort and improves the transient performance especially at start-ups.

In spite of a simple structure, the transport delay-based PLL provides a good synchronization capability in the case of ideal sinusoidal voltages. However in presence of harmonic components, its performance is highly degraded. The Hilbert transformation-based PLL as well as the all-pass filter-based PLL provides some kind of filtering and consequently presents a better harmonics rejection performance. The inverse Park PLL [66], illustrated in Fig. 6, and the SOGI PLL which uses the SOGI block for the fictitious phase generation [58] are two advanced single-phase PLLs with promising features including ease of implementation, robustness against disturbances, and frequency adaptive performance. Despite the wide acceptance and use of these two PLLs, the tuning of their parameters is not straightforward and is a trade-off between the bandwidth and the robustness and usually depends on the intended application [67,68].

5. Performance comparison

Computer simulations in MATLAB/Simulink were conducted for all three current control structures in order to present a performance comparison under different situations. Also, experimental verifications have been performed based on a TMS320F28335 digital signal controller from Texas Instruments. The block diagram of the studied single-phase grid connected converter is shown in Fig. 1.

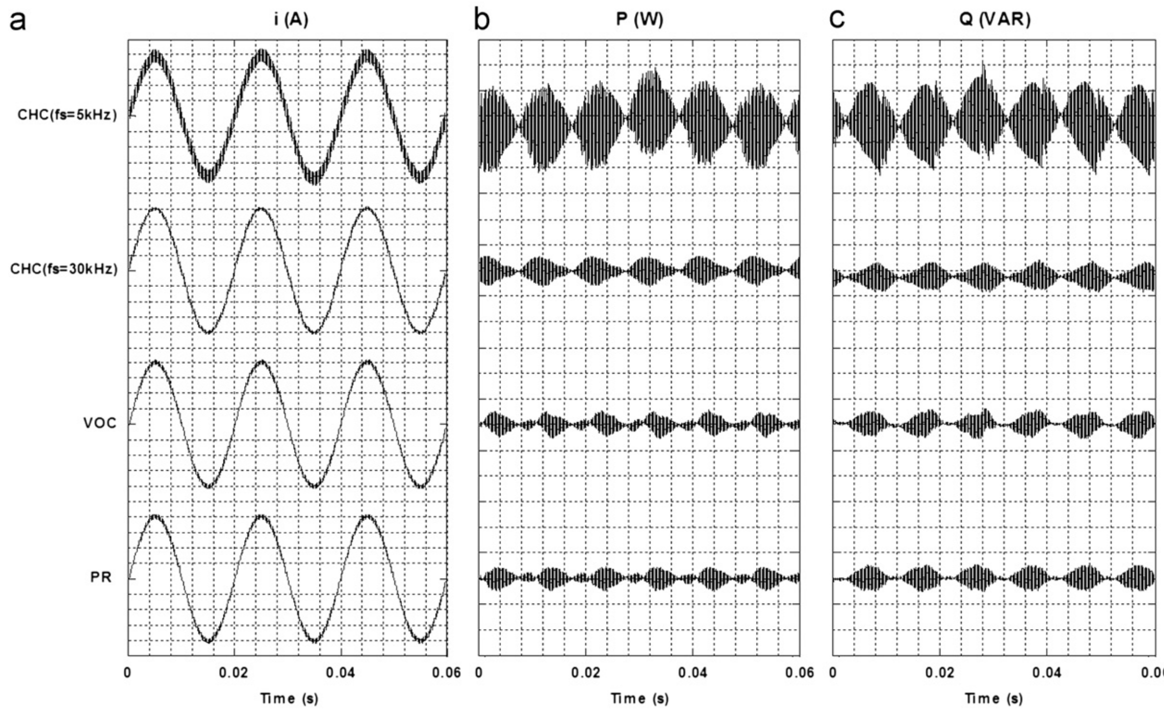


Fig. 8. Steady-state waveforms (P_{ref}=1000 W,Q_{ref}=0): (a) ac current (5 A/div), (b) active power (100 W/div) and (c) reactive power (100 VAR/div).

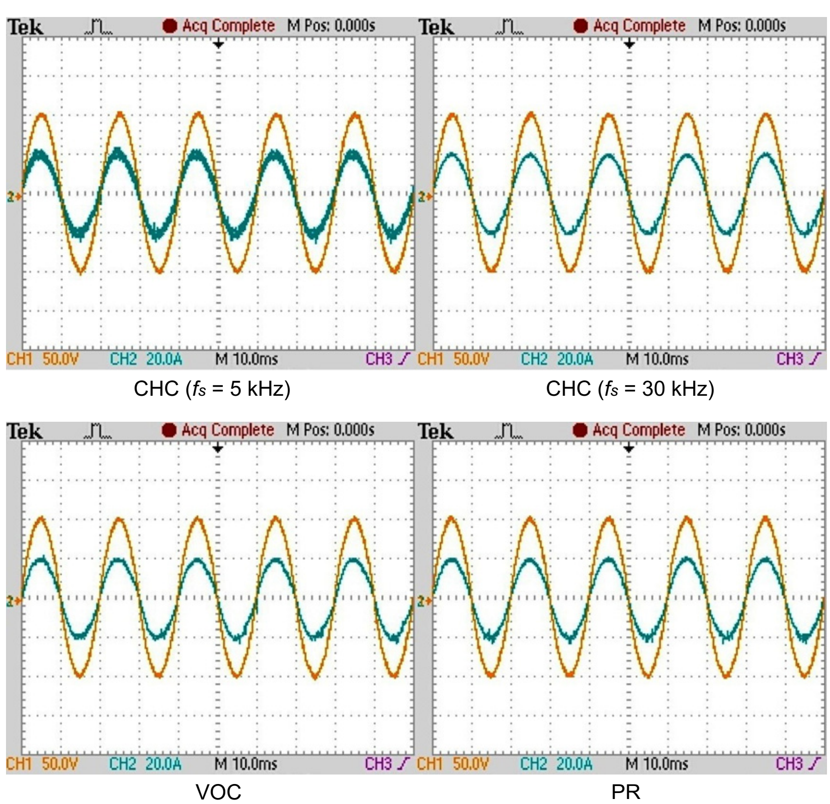


Fig. 9. Experimental steady-state waveforms (P_{ref}=1000 W,Q_{ref}=0); Ch1: grid voltage, and Ch2: ac current.

In simulations, the dc link is replaced with a constant dc supply and in experimental, a Chroma 6260 DC power supply is used to provide the constant dc link voltage. The current controller is picked from the structures demonstrated in Fig. 2. System parameters are the same for all studied control systems and are summarized in Table 1. A first-order APF, Eq. (12), is used for fictitious phase generation (if necessary) and for synchronization. The realization of Eq. (12) is shown in Fig. 7. To ensure the discrete accuracy, the trapezoidal method has been used for discretizing the continuous system in both computer simulation and experiments. Experimental results are obtained with the same parameters used in simulations. For the CHC method, the hysteresis bandwidth is selected such that the desired average switching frequency is achieved at the nominal conditions. The average converter switching frequency f_s is defined as $f_s=N_s/T_f$, where N_s is the number of switching operations for one leg of the converter in one fundamental period (T_f).

5.1. Steady-state and transient performance

The steady-state waveforms, the ac current trajectory and harmonic spectrum are presented in Figs. 8–11. The steady-state waveforms of the VOC and PR show superiority in providing more precise current control with less harmonic distortions (THD*i*) as well as more accurate regulation and less oscillations in the active and reactive powers. Figs. 8 and 9 show good agreement between simulations and experimental results. As it can be observed in Fig. 10, the ac current and its fictitious component retain the required circular shape of the trajectory. From Fig. 11, as it was expected, the VOC and PR have a similar harmonic spectrum.

In the case of CHC, an acceptable performance is only achieved when the hysteresis bandwidth is quite narrow. This narrow bandwidth translates to a high average converter switching frequency (f_s) and increased switching losses. For such a high average switching frequency, the CHC control quality is comparable to the VOC and PR techniques. Comparing Fig. 11(a) and (b), one can conclude that the current harmonics are mainly at multiples of average switching frequency and sampling frequency. When 4the narrower the hysteresis bandwidth is, the higher is the average switching frequency, better THD*i* is obtained and less low frequency harmonics are propagated to the ac source. These are at the expense of increased switching losses and EMI problems.

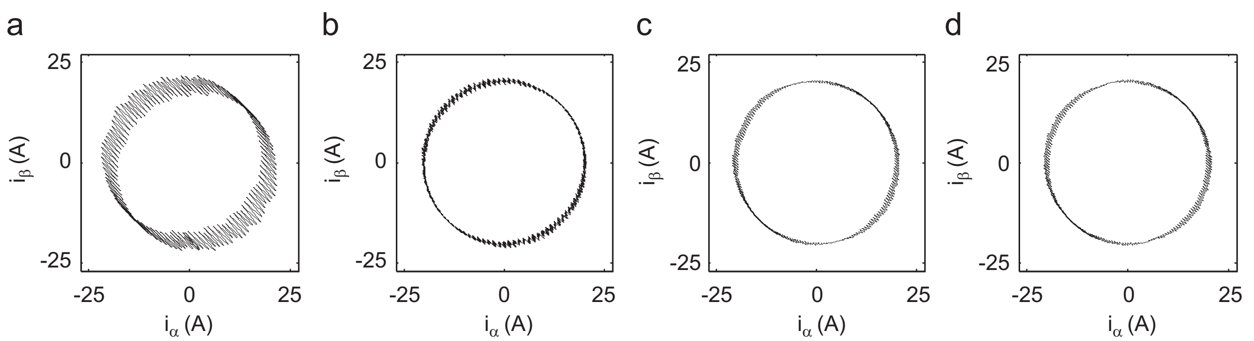


Fig. 10. AC current trajectory in steady-state and during one grid cycle (P_{ref}=1000W, Q_{ref}=0): (a) CHC (f_s=5 kHz), (b) CHC (f_s=30 kHz), (c) VOC and (d) PR.

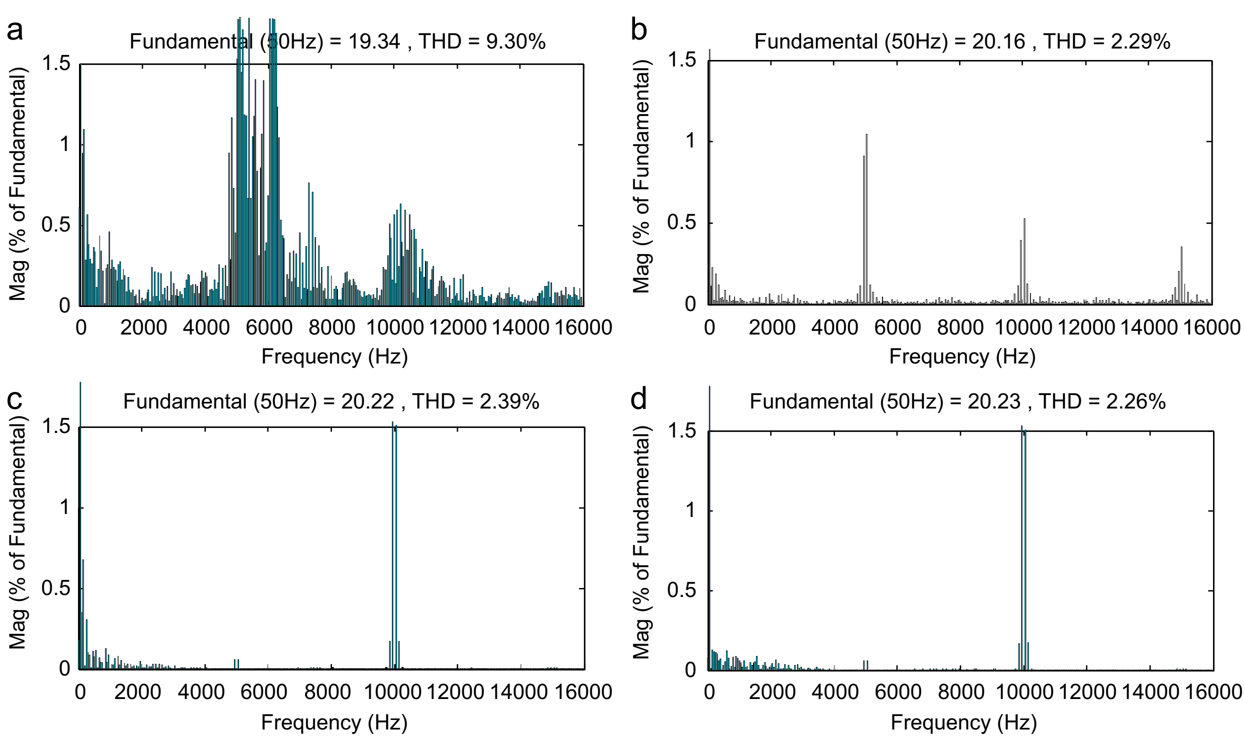


Fig. 11. AC current harmonic spectrum (P_{ref}=1000 W, Q_{ref}=0): (a) CHC (f_s=5 kHz), (b) CHC (f_s=30 kHz), (c) VOC and (d) PR.

Figs. 12 and 13 show the responses of the three control structures to various step changes in the active and reactive power references. It can be seen that the decoupling control of the active and reactive powers is slightly better for the VOC with the decoupling feedforward terms.

5.2. Effect of switching frequency and filter inductance on THDi

Voltage source converters are connected to the grid through a passive filter to suppress high frequency switching ripples. A simple inductor is the most common form of a passive filter

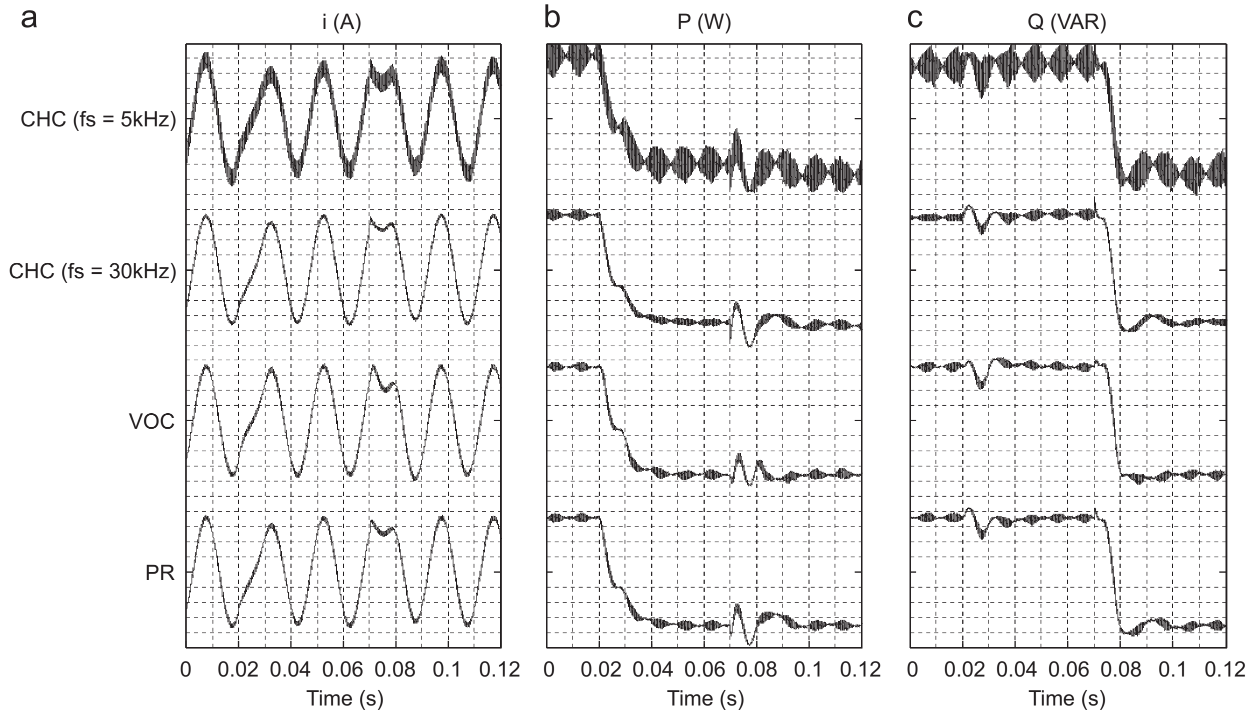


Fig. 12. Transient response for step changes of active and reactive power references from 500 W (VAR) to −500 W (VAR) at 0.02 s (0.07 s): (a) ac current (4A/div), (b) active power (200 W/div) and (c) reactive power (200 VAR/div).

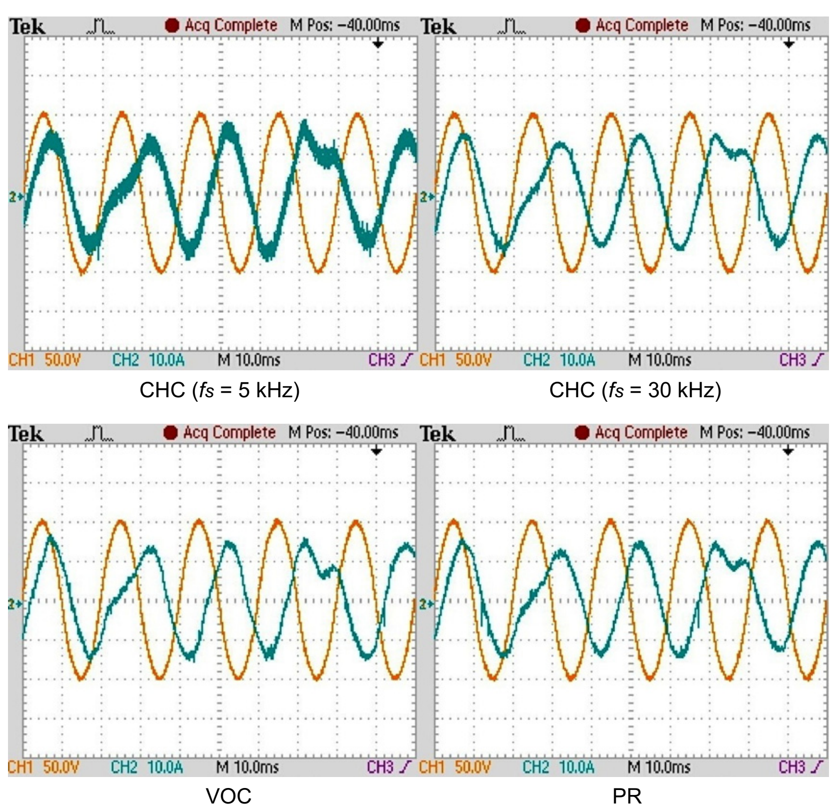


Fig. 13. Experimental waveforms for transient response for step changes of active and reactive power references from 500 W (VAR) to −500 W (VAR) at 0.02 s (0.07 s); Ch1: grid voltage, and Ch2: ac current.

utilized for the grid integration of power converters. By increasing the switching frequency, the switching ripples transfer to higher frequencies and consequently a smaller inductance is needed to mitigate them. The switching losses limit the maximum allowed switching frequency, while the fundamental voltage drop limits the size of filter inductance. When designing a grid connected converter, there should be a satisfactory tradeoff between the maximum switching frequency and the size of the filter inductance to comply with standards, such as IEEE519 [69].

In this subsection, the effect of switching frequency and filter inductance on the ac current total harmonic distortion for three different control strategies is studied. The results are summarized in Fig. 14. Obviously, both filter inductance and switching frequency have considerable impact on the THD*i*. In the case of CHC, the converter average switching frequency should be very high in order to sufficiently attenuate the converter harmonics. From Fig. 14(b) it can be concluded that for small switching frequencies, the VOC has a better performance in the term of THD*i* compared to the PR.

5.3. Effect of distorted line voltage on THDi

If the grid voltage is harmonically polluted which is the case for most of distribution networks, the current controller should be, to some extent immune, to the grid voltage harmonics which are mainly the 3rd and 5th in single-phase systems. In this study, 5th harmonic is imposed on the fundamental frequency voltage waveform. The results for three control strategies are depicted in Fig. 15. Again, the VOC, especially for higher harmonic penetrations, provides lower THD*i* values. If the application demands for more immunity to the grid voltage harmonics, more resonant terms can be readily added to the basic PR control structure as illustrates in (8). In this study, harmonic compensators (HCs) tuned at 3rd, 5th, and 7th harmonics are utilized. Although simple in principle and easy to realize, this solution can significantly improve the THD*i* in the presence of background voltage distortion, as illustrated in Fig. 15.

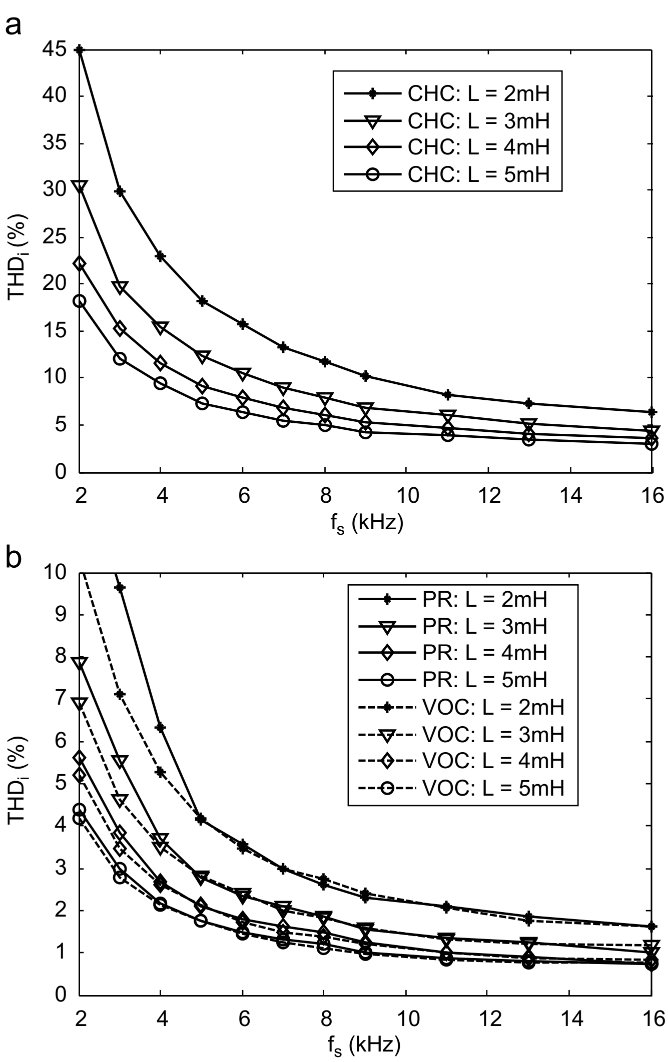


Fig. 14. Effect of switching frequency and filter inductance on THD*i* (P_{ref}=1000 W, Q_{ref}=0): (a) CHC, and (b) VOC and PR.

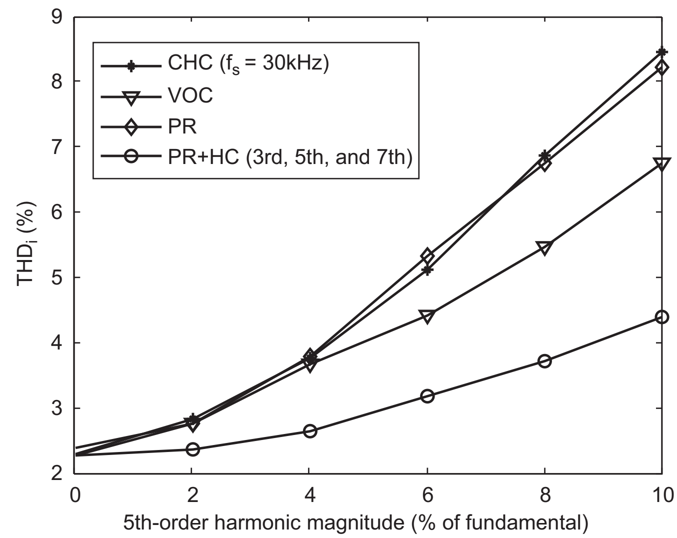


Fig. 15. Effect of distorted line voltage on THD*i* (P_{ref}=1000 W and Q_{ref}=0).

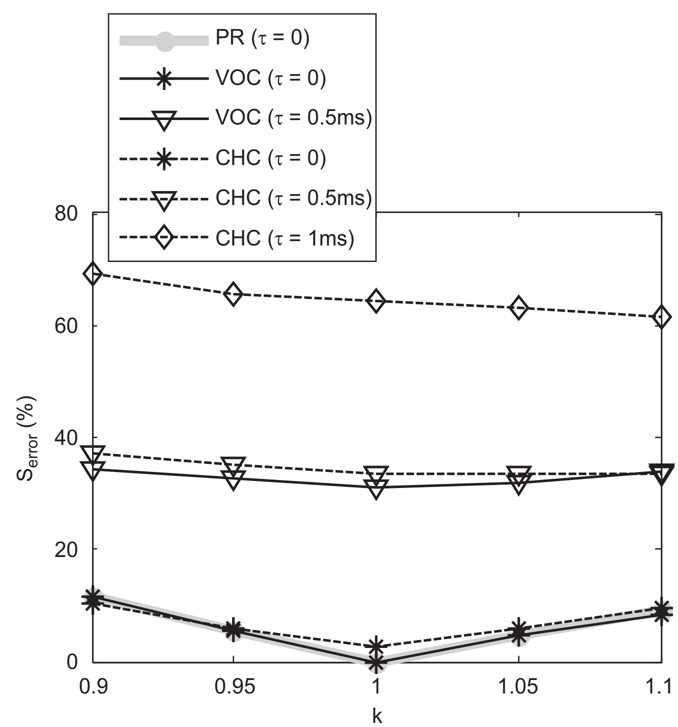


Fig. 16. Effect of current measurement error on steady-state performance (P_{ref}=1000 W and Q_{ref}=0).

Table 2
Performance comparison of different control techniques for single-phase grid-tie converters.

	Advantages	Disadvantages
CHC	– Simple; requires almost no information about the system, and has no parameter to tune – no separate PWM block – no need for fictitious phase information of voltage or current in the current control loop – easy to realize with analog or digital systems	– Widely variable switching frequency, especially when the average switching frequency is not too high, which results in difficulty when designing the filter and power circuit – to achieve a good performance, high values for the average switching frequency and the filter inductance are necessary
VOC	– Less control effort and fast and smooth startup thanks to the feedforward voltages – fixed switching frequency and possibility of using advanced modulation techniques – lowest THD*i* at small switching frequencies among all compared techniques – lowest THD*i* at highly disturbed ac voltages among all compared techniques (except for PR-HC) – lowest coupling between active and reactive powers control thanks to the decoupling network	– Complex structure including two PI controllers, a decoupling network, and reference frame transformations – a strong coupling between control variables (I_d, I_q) which requires a decoupling network – requires the value of filter inductance in the decoupling network – requires fictitious phase information of both voltage and current in the current control loop
PR (PR-HC)	– Relatively simple – fixed switching frequency and possibility of using advanced modulation techniques – simplicity of selective harmonic compensation, especially for low-order harmonics – no need for fictitious phase information of voltage or current in the current control loop	– Sensitivity to system frequency variations; requires a frequency feedback from the PLL to enhance the performance – great sensitivity and possibility of instability to the phase shift of current sensors

5.4. Effect of current measurement error

In a real application, due to some practical issues such as signal acquisition and filtering, A/D distortions, scaling errors, etc., phase shift and magnitude errors may occur in the measured ac current. To study this problem, it is assumed that the measured current have both amplitude deviation, denoted by k, and time delay, expressed by τ, with respect to the real current, as stated in (13).

$$i_{meas}(t) = k i_{real}(t+\tau) \tag{13}$$

The performance of CHC (f_s=30 kHz), VOC, and PR control systems considering the measurement error in the ac current is investigated for different values of k and τ and results are presented in Fig. 16, in which S_{error} (%) is defined by

$$S_{error}(\%) = \sqrt{\frac{(P-P_{ref})^2+(Q-Q_{ref})^2}{P_{ref}^2+Q_{ref}^2}} \times 100 \tag{14}$$

Clearly, the effect of amplitude error is not substantial, while the time delay (equivalent as a phase shift in the frequency domain) significantly affects the performance. The CHC is more robust than others against the phase shift in the measured current. Even with considerable long time delays, which are not likely in practical applications, the system remains stable; however the power regulation error increases drastically. The VOC can also tolerate a long delay as 0.5 ms and beyond this it becomes unstable. The PR presents great sensitivity and becomes unstable even with a very small time delay in the measured current.

6. Conclusions

From the above conducted studies, one can conclude that if wisely designed, both VOC and PR present similar steady-state and transient performances and can successfully achieve accurate regulation with fast dynamic response with minimum overshoot and harmonic distortions. The same performance can be achieved with the CHC only when the average switching frequency and as a consequence the switching losses are quite high. On the other hand, in spite of three-phase systems, where the instantaneous powers are regulated, the controlled variables in single-phase converters are the average powers, so the overall control system including the power and current control loops has a relatively slow dynamics. Therefore, the high dynamic, characterized as the main advantage of the CHC in three-phase applications, does not anymore represent any efficiency in a single-phase system with slow dynamics. On the other hand, for low switching frequencies or disturbed line voltages, the VOC shows a better performance in terms of THD*i*. A promising feature of the PR control is its flexibility for selective harmonic compensation, especially for low-order harmonics, which makes it an ideal solution for the applications where high system dynamics and harmonics compensation are required at the same time. A comparison among all studied techniques is presented in Table 2. It is generally concluded that, the PR-based technique is an interesting alternative of the VOC for single-phase grid integration of small-scale renewable energy sources. The most important concern about a PR controller is its great sensitivity and possibility of instability to the phase shift of current sensors. To overcome this problem, high bandwidth current sensors should be utilized with a PR controlled converter. Also, phase shifts in the monitored ac current, mainly introduced by low pass filters, should be properly compensated prior to feeding the current to the controller.

References

[1] Akorede MF, Hizam H, Ab Kadir MZA, Aris I, Buba SD. Mitigating the anthropogenic global warming in the electric power industry. Renewable and Sustainable Energy Reviews 2012;16:2747–61 (June (5)).

[2] Moriarty P, Honnery D. What is the global potential for renewable energy? Renewable and Sustainable Energy Reviews 2012;16:244–52 (January (1)).
[3] Lund PD. Boosting new renewable technologies towards grid parity—economic and policy aspects. Renewable Energy 2011;36:2776–84 (November (11)).
[4] European Renewable Energy Council (EREC). Renewable Energy Scenario to 2040, Half of the Global Energy Supply From Renewable in 2040. Available at 〈http://www.erec-renewables.org〉.
[5] Tolón-Becerra A, Lastra-Bravo X, Bienvenido-Bárcena F. Proposal for territorial distribution of the EU 2020 political renewable energy goal. Renewable Energy 2011;36:2067–77 (August (8)).
[6] Vithayasrichareon P, MacGill IF, Nakawiro T. Assessing the sustainability challenges for electricity industries in ASEAN newly industrialising countries. Renewable and Sustainable Energy Reviews 2012;16:2217–33 (May (4)).
[7] Pereira Jr. AO, Pereira AS, Rovere ELL, Barata MML, Villar SC, Pires SH. Strategies to promote renewable energy in Brazil. Renewable and Sustainable Energy Reviews 2011;15:681–8 (January (1)).
[8] Nautiyal HVarun. Progress in renewable energy under clean development mechanism in India. Renewable and Sustainable Energy Reviews 2012;16: 2913–9 (June (5)).
[9] Malik SN, Sukhera OR. Management of natural gas resources and search for alternative renewable energy resources: a case study of Pakistan. Renewable and Sustainable Energy Reviews 2012;16:1282–90 (February (2)).
[10] Yuan J, Kang J, Yu C, Hu Z. Energy conservation and emissions reduction in China-progress and prospective. Renewable and Sustainable Energy Reviews 2011;15:4334–47 (December (9)).
[11] Hasan MH, Muzammil WK, Mahlia TMI, Jannifar A, Hasanuddin I. A review on the pattern of electricity generation and emission in Indonesia from 1987 to 2009. Renewable and Sustainable Energy Reviews 2012;16:3206–19 (June (5)).
[12] Shafie SM, Mahlia TMI, Masjuki HH, Andriyana A. Current energy usage and sustainable energy in Malaysia: a review. Renewable and Sustainable Energy Reviews 2011;15:4370–7 (December (9)).
[13] Sawangphol N, Pharino C. Status and outlook for Thailand's low carbon electricity development. Renewable and Sustainable Energy Reviews 2011;15:564–73 January (1)).
[14] Abanda FH, Ng'ombe A, Keivani R, Tah JHM. The link between renewable energy production and gross domestic product in Africa: a comparative study between 1980 and 2008. Renewable and Sustainable Energy Reviews 2012;16:2147–53 (May (4)).
[15] Kaundinya DP, Balachandra P, Ravindranath NH. Grid-connected versus stand-alone energy systems for decentralized power—a review of literature. Renewable and Sustainable Energy Reviews 2009;13:2041–50 (October (8)).
[16] Akorede MF, Hizam H, Pouresmaeil E. Distributed energy resources and benefits to the environment. Renewable and Sustainable Energy Reviews 2010;14:724–34 (February (2)).
[17] Ichikawa R, Funato H, Nemoto K. Experimental verification of single phase utility interface inverter based on digital hysteresis current controller. Electrical Machines and Systems (ICEMS) 2011:1–6.
[18] Dahono PA. New hysteresis current controller for single-phase full-bridge inverters. Power Electronics, IET 2009; 2 (September (5)): 585–594.
[19] Azab M. A new direct power control of single phase PWM boost converter. In: Circuits and Systems. 46th IEEE Midwest Symposium 2003; p. 1081–1084.
[20] Indu Rani B, Saravana Ilango G, Nagamani C. Power flow management algorithm for photovoltaic systems feeding DC/AC loads. Renewable Energy 2012;43:267–75 (July (1)).
[21] Zang H, Yang X. Simulation of two-level photovoltaic grid-connected system based on current control of hysteresis band. In: Power and Energy Engineering Conference (APPEEC) Asia-Pacific 2011; p. 1–4.
[22] Yao Z, Xiao L. Control of single-phase grid-connected inverters with nonlinear loads. IEEE Transactions on Industrial Electronics 2012:99.
[23] Yao Z, Xiao L, Yan Y. Seamless transfer of single-phase grid-interactive inverters between grid-connected and stand-alone modes. IEEE Transactions on Power Electronics 2010;25:1597–603 (June (6)).
[24] Elsaharty MA, Hamad MS, Ashour HA. Digital hysteresis current control for grid-connected converters with LCL filter. In: 37th Annual Conference on IEEE Industrial Electronics Society (IECON 2011) 2011; p. 4685–4690.
[25] Calais M, Agelidis VG, Dymond MS. A cascaded inverter for transformerless single- phase grid-connected photovoltaic systems. Renewable Energy 2001;22:255–62 (January–March (1–3)).
[26] Dai X, Chao Q. The research of photovoltaic grid-connected inverter based on adaptive current hysteresis band control scheme. In: International Conference on Sustainable Power Generation and Supply (SUPERGEN 09) 2009; p. 1–8.
[27] Bahrani B, Rufer A, Kenzelmann S, Lopes LAC. Vector control of single-phase voltage-source converters based on fictive-axis emulation. IEEE Transactions on Industrial Applications 2011;47:831–40 (March/April (2)).
[28] Miranda UA, Rolim LGB, Aredes MA. DQ synchronous reference frame current control for single-phase converters. In: Power electronics specialists conference 2005; p. 1377–1381.
[29] Gong JW, Chen BF, Li P, Liu F, Zha XM. Feedback decoupling and distortion correction based reactive compensation control for single-phase inverter. Power Electronics and Drive Systems (PEDS) 2009:1454–9.
[30] Samerchur S, Premrudeepreechacharn S, Kumsuwun Y, Higuchi K. Power control of single-phase voltage source inverter for grid-connected photovoltaic systems. In: Power systems conference and exposition (PSCE) 2011; p. 1–6.
[31] Amin MMN, Mohammed OA. Vector oriented control of voltage source PWM inverter as a dynamic VAR compensator for wind energy conversion system connected to utility grid. In: Applied power electronics conference and exposition (APEC) 2010; p. 1640–1650.
[32] Ciobotaru M, Teodorescu R, Blaabjerg F. Control of single-stage single-phase PV inverter. Power Electronics and Applications 2005:1–10.
[33] Jiabing H, Yikang H. DFIG wind generation systems operating with limited converter rating considered under unbalanced network conditions—analysis and control design. Renewable Energy 2011;36:829–47 (February (2)).
[34] Barote L, Marinescu C. Current control of single-phase inverter for wind turbine applications. Advanced Topics in Electrical Engineering (ATEE) 2011:1–4.
[35] Tao H, Duarte JL, Hendrix MAM. Line-interactive UPS using a fuel cell as the primary source. IEEE Transactions on Industrial Electronics 2008;55:3012–21 (August (8)).
[36] Castilla M, Miret J, Matas J, Vicuna LG, Guerrero JM. Control design guidelines for single-phase grid-connected photovoltaic inverters with damped resonant harmonic compensators. IEEE Transactions on Industrial Electronics 2009;56:4492–501 (November (11)).
[37] Castilla M, Miret J, Matas J, Vicua LG, Guerrero JM. Linear current control scheme with series resonant harmonic compensator for single-phase grid-connected photovoltaic inverters. IEEE Transactions on Industrial Electronics 2008;55:2724–33 (July (7)).
[38] He J, Li Y. Hybrid voltage and current control approach for DG-grid interfacing converters with LCL filters. IEEE Transactions on Industrial Electronics 2012:99.
[39] Jung E, Sul SK Implementation of grid-connected single-phase inverter based on FPGA. In: Applied power electronics conference and exposition (APEC 2009) 2009; p. 889–893.
[40] Peng S, Luo A, Chen Y, Lv Z. Dual-loop power control for single-phase grid-connected converters with LCL filter. Journal of Power Electronics 2011;11:456–63 (July (4)).
[41] Guofei T, Guochun X, Zhibo Z, Yong L A control method with grid disturbances suppression for a single-phase LCL-filter-based grid-connected inverter. In: Applied power electronics conference and exposition (APEC) 2012; p. 1489–1493.
[42] Kojabadi HM, Yu B, Gadoura IA, Chang L, Ghribi M. A novel DSP-based current-controlled PWM strategy for single phase grid connected inverters. IEEE Transactions on Power Electronics 2006:985–93 l.21 (July (4)).
[43] Gow JA, Manning CD. Novel fast-acting predictive current mode controller for power electronic converters. Electric Power Applications 2001:133–9.
[44] Yu B, Chang L. Improved predictive current controlled PWM for single-phase grid-connected voltage source inverters. In: Power electronics specialists conference (PESC 05) 2005; p. 231–236.
[45] Premrudeepreechacharn S, Poapornsawan T. Fuzzy logic control of predictive current control for grid-connected single phase inverter. In: Photovoltaic specialists conference 2000; p. 1715–1718.
[46] Viola J, Restrepo J, Diaz M, Aller JM, Harley RG, Habetler TG. Simplified control structure for current control of single phase rectifiers using COT-ANN-PWM. In: International joint conference on neural networks 2007; p. 1370–1374.
[47] Yang W, Li M. Design and simulation of single phase photovoltaic grid-connected system based on quasi-sliding mode control. Control, Automation and Systems Engineering (CASE) 2011:1–4.
[48] Kim IS. Sliding mode controller for the single-phase grid-connected photovoltaic system. Applied Energy 2006;83:1101–15 (October (10)).
[49] Xuesong Z, Daichun S, Youjie M, Deshu C. Grid-connected control and simulation of single-phase two-level photovoltaic power generation system based on repetitive control. In: International conference on measuring technology and mechatronics automation (ICMTMA). 2010; p. 366–369.
[50] Bojoi R, Roiu D, Griva G, Tenconi A. Single-phase grid-connected distributed generation system with maximum power tracking. In: International conference on optimization of electrical and electronic equipment (OPTIM) 2010; p. 1131–1137.
[51] Dasgupta S, Sahoo SK, Panda SK. Single-phase inverter control techniques for interfacing renewable energy sources with microgrid-Part I: Parallel-connected inverter topology with active and reactive power flow control along with grid current shaping. IEEE Transactions on Power Electronics 2011;26:717–31 (March (3)).
[52] Dasgupta S, Sahoo SK, Panda SK. Amaratunga GAJ. Single-phase inverter-control techniques for interfacing renewable energy sources with microgrid-Part II: series-connected inverter topology to mitigate voltage-related problems along with active power flow control. IEEE Transactions on Power Electronics 2011;26:732–46 (March (3)).
[53] Bojoi R, Limongi LR, Roiu D, Tenconi A. Enhanced power quality control strategy for single-phase inverters in distributed generation systems. In: 2010 IEEE International Symposium on Industrial Electronics (ISIE) 2010; p. 2727–2732.
[54] Sakamoto S, Izumi T, Yokoyama T, Haneyoshi T. A new method for digital PLL control using estimated quadrature two phase frequency detection. In: Power conversion conference 2002; p. 671–676.
[55] Saitou M, Shimizu T. Generalized theory of instantaneous active and reactive powers in single-phase circuits based on Hilbert transform. In: Power electronics specialists conference 2002; p. 1419–1424.
[56] Saitou M, Matsui N, Shimizu T. A control strategy of single-phase active filter using a novel d-q transformation. In: Industry applications conference 2003; p. 1222–1227.
[57] Kwon BH, Choi JH, Kim TW. Improved single-phase line-interactive UPS. IEEE Transactions on Industrial Electronics 2001;48:804–11 (August (4)).

[58] Ciobotaru M, Teodorescu R, Blaabjerg F. A new single-phase PLL structure based on second order generalized integrator. In: Power electronics specialists conference 2006; p. 1–6.
[59] Dong D, Thacker T, Cvetkovic I, Burgos R, Boroyevich D, Wang FF, et al. Modes of operation and system-level control of single-phase bidirectional PWM converter for microgrid systems. IEEE Transactions on Smart Grid 2012;99:PP 1–12.
[60] Tseng CC, Pei SC. Design and application of discrete-time fractional Hilbert transformer. IEEE Transactions on Circuits and Systems II: Analog and Digital Signal Processing 2000;47:1529–33 (December (12)).
[61] Blaabjerg F, Teodorescu R, Liserre M, Timbus AV. Overview of control and grid synchronization for distributed power generation systems. IEEE Transactions on Industrial Electronics 2006;53:1398–409 (October (5)).
[62] Santos Filho RM, Seixas PF, Cortizo PC, Torres LAB, Souza AF. Comparison of three single-phase PLL algorithms for UPS applications. IEEE Transactions on Industrial Electronics 2008;55:2923–32 (August (8)).
[63] Silva SM, Lopes BM, Filho BJC, Campana RP, Bosventura WC. Performance evaluation of PLL algorithms for single-phase grid-connected systems. In: Industry applications conference 2004; p. 2259–2263.
[64] Nicastri A, Nagliero A. Comparison and evaluation of the PLL techniques for the design of the grid-connected inverter systems. Industrial Electronics (ISIE) 2010:3865–70.
[65] Thacker T, Boroyevich D, Burgos R, Wang F. Phase-locked loop noise reduction via phase detector implementation for single-phase systems. IEEE Transactions on Industrial Electronics 2011;58:2482–90 (June (6)).
[66] Arruda LN, Silva SM, Filho BJC PLL. Structures for utility connected systems. In: Industry applications conference 2001; p. 2655–2660.
[67] Ferreira RJ, Araujo RE, Pecas Lopes JA. A comparative analysis and implementation of various PLL techniques applied to single-phase grids. In: International youth conference on energetics (IYCE) 2011; p. 1–8.
[68] Golestan S, Monfared M, Freijedo F, Guerrero J. Design and tuning of a modified power-based PLL for single-phase grid-connected power conditioning systems. IEEE Transactions on Power Electronics 2012; PP (99).
[69] IEEE Recommended Practices and Requirements for Harmonic Control in Electrical Power Systems. IEEE Std 519-1992.